



Published in final edited form as:

J Comp Neurol. 2011 June 1; 519(8): 1562–1579. doi:10.1002/cne.22585.

Formation of the spinal network in zebrafish determined by domain-specific *Pax* genes

Takanori Ikenaga¹, Jason M. Urban¹, Nichole Gebhart², Kohei Hatta³, Koichi Kawakami^{4,5}, and Fumihito Ono¹

¹Laboratory of Molecular Physiology, National Institute on Alcohol Abuse and Alcoholism, National Institutes of Health, Bethesda, MD, 20892, USA

²The Whitney Laboratory for Marine Bioscience, University of Florida, St Augustine, FL, 32080, USA

³Graduate School of Life Science, University of Hyogo, 3-2-1 Kouto, Kamigori, Ako-gun, Hyogo 678-1297, Japan

⁴Division of Molecular and Developmental Biology, National Institute of Genetics

⁵Department of Genetics, The Graduate University for Advanced Studies (SOKENDAI), 1111 Yata, Mishima, Shizuoka 411-8540, Japan

Abstract

In the formation of the spinal network, various transcription factors interact to develop specific cell types. Using a gene trap technique, we established a stable line of zebrafish in which the red fluorescent protein (RFP) was inserted in the *pax8* gene. RFP insertion marked putative *pax8*-lineage cells with fluorescence and inhibited *pax8* expression in homozygous embryos. *Pax8* homozygous embryos displayed defects in the otic vesicle, as previously reported in studies using morpholinos. The *pax8* homozygous embryos survived to adulthood in contrast to mammalian counterparts that die prematurely. RFP is expressed in the dorsal spinal cord. Examination of the axon morphology revealed that RFP (+) neurons include Commissural Bifurcating Longitudinal (CoBL) interneurons, but other inhibitory neurons such as Commissural Local (CoLo) interneurons and Circumferential Ascending (CiA) interneurons do not express RFP. We examined the effect of inhibiting *pax2a/pax8* expression on interneuron development. In *pax8* homozygous fish, the RFP (+) cells undergo differentiation similar to that of *pax8* heterozygous fish, and the swimming behavior remained intact. In contrast, the RFP (+) cells of *pax2a/pax8* double mutants displayed altered cell fates. CoBLs were not observed. Instead, RFP (+) cells exhibited axons descending ipsilaterally: a morphology resembling that of V2a/V2b interneurons.

Keywords

Spinal cord; Transcription factor; Differentiation; Gene trap; Cell fate; Paired box gene

Corresponding Author: Fumihito Ono, Laboratory of Molecular Physiology, National Institute on Alcohol Abuse and Alcoholism, National Institutes of Health, Bethesda, MD, 20892, USA. onof@mail.nih.gov.

Supporting grant information: This research was supported by NINDS Grant 1R01NS050388-01A1 to FO, Muscular Dystrophy Association Grant MDA3818 to FO, and the intramural research program of the NIH/NIAAA.

Introduction

Pax8 is a transcription factor that belongs to the *Pax* gene family. *Pax* genes are homologues of the *Drosophila* gene *paired* (Treisman et al., 1991), which is involved in the pair-rule segmentation. The *Pax* gene is characterized by the existence of a paired domain, which is comprised of two sub-domains, with each of these domains having the ability to bind to DNA. Genes in this family play important roles in various aspects of development (Chi and Epstein, 2002). *Pax2*, *Pax5* and *Pax8* constitute a subfamily of the *Pax* genes. *Pax8* has been cloned from zebrafish (Pfeffer et al., 1998; Mackereth et al., 2005), and its expression was detected in similar organs as in mammals (Bouchard et al., 2004).

A null mutant of *pax8* was never isolated in a large-scale mutagenesis screening of zebrafish. To date several studies have used morpholinos (MOs) to knockdown Pax8 (Hans et al., 2004; Mackereth et al., 2005). In these studies, injection of *pax8* MOs resulted in a decrease in size of the otic vesicle at 30 hours post-fertilization (hpf).

The expression of transcription factors and the regulation of cell fates in the spinal cord have been studied extensively in mammals (Burrill et al., 1997; Jessell, 2000; Goulding and Pfaff, 2005). Several genes of the *Pax* family have been found to be involved in these processes. *Pax2* is expressed in postmitotic cells in the lateral portion of the spinal cord (Burrill et al., 1997). *Pax6* establishes distinct ventral cell populations and controls identity of motor neurons and interneurons (Ericson et al., 1997). Studies in zebrafish are less comprehensive compared to that of mammals. However, in several studies, the identity of neurons in the spinal cord was clearly linked to the expression of transcription factors. *Engrailed-1*-expressing neurons are ipsilateral ascending glycinergic inhibitory neurons (Higashijima et al., 2004) and *alx*-expressing neurons are ipsilateral descending glutamatergic neurons (Kimura et al., 2006). Transcription factors including *islet1*, *islet2*, and *nkx6* are important for the development of primary motor neurons (Segawa et al., 2001; Hutchinson and Eisen, 2006; Hutchinson et al., 2007).

Gene trap screening, widely used in *Drosophila* and mouse, is a genetic technique used to identify gene expression and function (O’Kane and Gehring, 1987; Friedrich and Soriano, 1991). It has only recently been applied to zebrafish (Kawakami et al., 2004). In our gene trap screening, using the red fluorescent protein (RFP), we identified a line in which the RFP gene was inserted in the *pax8* gene. The insertion of RFP occurred in the first intron of *pax8*, leading to a fusion transcript between *pax8* and RFP. We used this fish to analyze RFP (+) neurons in developing zebrafish. Embryos homozygous for the insertion had a very low *pax8* transcript level, rendering the fish a *pax8* hypomorph. Analysis of RFP (+) neurons in the spinal cord revealed that a subpopulation of inhibitory interneurons arose from the putative *pax8*-lineage. The analysis of *pax2/pax8* double mutants revealed an interaction of *pax8* and *pax2a* in the differentiation of putative *pax8*-lineage neurons.

Material and Methods

Maintenance of zebrafish lines

Wild type zebrafish were obtained from Aquatic Ecosystems, and maintained in stand-alone self-circulating AHAB systems (Aquatic Ecosystems, Apopka, FL) following the guidelines of IACUC at the University of Florida (protocol #D464) and NIH/NIAAA (protocol #LMP-FO-11). Both protocols conformed to the NIH Guidelines for Use of Zebrafish. A founder fish harboring the RFP insertion in the *pax8* gene (F0) was out-crossed with wild type fish for several generations. F3 and later generations were used for experiments. Embryos were maintained at 28.5°C. *Noi* mutant (*noi*^{b593}) (Erickson et al., 2007), a mutant of *pax2a*, was obtained from the Zebrafish International Resource Center.

Gene trap screening and mapping of the insertion site

The GFP sequence between the BamHI site and the NotI site of the clone pT2KSAG (Kawakami et al., 2004) was cut out and the sequence of DsRedExpress (BD, Franklin Lakes, NJ) was inserted in its place. The plasmid, named Tol2-DsRed, was used for injection into zebrafish eggs.

Transposase mRNA was prepared from pCS-TP (Kawakami et al., 2004) using the mMessage mMachine SP6 kit (Ambion, Austin, TX). Tol2DsRed plasmid and transposase was diluted to a final concentration of 50 ng/ μ l. Injection into fertilized zebrafish eggs was performed as previously described (Ono et al., 2001). Surviving embryos were raised to adulthood. They were in-crossed or out-crossed with wild type fish to screen for RFP (+) fish. Screening of fish was done between 72 hpf to 120 hpf.

Inverse PCR was performed following the protocol described in Kawakami et al. (2004) with slight modifications. To determine the site of insertion, amplified products were directly sequenced and used to search the zebrafish genomic database (Sanger) using BLAST.

Real-time PCR (qPCR)

RNA was extracted from 24 hpf embryos and 10 days post fertilization (dpf) larvae, using RNeasy mini kit (Qiagen, Valencia, CA). RNA samples were treated with TurboDNase (Ambion). Total RNA was reverse transcribed using iScript cDNA Synthesis Kit (Bio-Rad, Hercules, CA), followed by RNase treatment. *Pax8* primers and probe were designed to amplify the junction of exons 5 and 6; forward 5'-AAG TGC AGC AGC CAT TTA ACC TCC-3', reverse 5'-TTG ATG GAG TAA GTG GAG CCC AGA-3', FAM labeled probe/56-FAM/TAA AGG CCT GAG CCC AGG ACA C/3BHG_1/(Integrated DNA Technologies, Coralville, IA). Exons 5 and 6 are present in all reported splicing isoforms of *pax8* (Mackereth et al., 2005).

qPCR was carried out with ABI StepOnePlus (ABI, Foster City, CA). Data was analyzed using the comparative C_t method (C_t) with elongation factor (*elf*) 1-alpha (NM_131263.1) as endogenous reference. Primers and probe for *elf*1-alpha were; forward 5'-TTG ATG CCC TTG ATG CCA TTC TGC-3', reverse 5'-ACA ACC ATA CCA GGC TTG AGG ACA-3' and probe/56-FAM/ATT GGC ACT GTA CCT GTG GGT CGT GT/3BHQ_1/.

Optical studies

Screening of RFP signals in zebrafish embryos was performed on the Olympus MVX fluorescent stereomicroscope. Images were recorded with Olympus DP70 Color CCD camera. Confocal microscopy imaging was done on a Zeiss confocal microscope 510 Meta with 25X or 40X water immersion objective or Olympus FV-300 with 40X water immersion objective. For double imaging of RFP and GFP, sequential scanings were performed. Images were imported into Photoshop (Adobe Systems, San Jose, CA) and analyzed. Size, contrast and brightness were adjusted in Photoshop.

Retrograde labeling of spinal interneurons and reticulo-spinal neurons

To visualize the spinal interneurons in *pax8* heterozygous (*pax8^{+/m}*) or *pax8* homozygous (*pax8^{m/m}*) fish, retrograde labeling with Alexa Fluor 488 conjugated dextran (3,000 MW, Invitrogen, Eugene, OR) was performed as previously described (Hale et al., 2001). In brief, fish were anesthetized in 0.1 g/l MS-222 (tricaine methanesulfonate, Sigma, St. Louis, MO) and placed onto an agar plate. Injection electrodes, with a tip diameter of ~15 μ m, were filled with 50% (v/v) Alexa Fluor 488 conjugated dextran solution and inserted into the spinal cord. After allowing a few seconds for the dye to diffuse, the electrode was

withdrawn. Fish were allowed to recover in a physiologically conditioned solution for at least 3 hours prior to confocal imaging.

For the retrograde labeling of reticulo-spinal neurons, fish were anesthetized and embedded in 2% low melting point agarose (melting point 25 ± 5 °C, Fisher Scientific, Pittsburgh, PA). A section of the fish trunk was exposed by removal of the surrounding agarose. This trunk section was then cut using a scalpel blade coated with dextran fluorescein (10,000 MW, Invitrogen). Following this procedure the fish were left in the agarose for 5 minutes to allow for the intake of dextran into the spinal cord. Post surgical recovery and confocal imaging were carried out as described previously.

Stochastic labeling of spinal interneurons

Stochastic labeling of the spinal interneurons in *pax8^{+/m}* or *pax8^{m/m}* fish was obtained by the injection of a(n) *eng1*-EGFP, HuC-GFP, or EF-GVP-Ulny-UH2B construct at 1–64 cell stage. The EF-GVP-Ulny-UH2B construct is comprised of three genes: Gal4-VP16 following the *Xenopus* EF-1 α -promoter, lynEGFP following the 14xUAS-E1b promoter and H2B-EYFP following the 14xUAS-E1b promoter (Koster and Fraser, 2001). LynEGFP encodes EGFP localized to the membrane, and H2B-EYFP encodes EYFP localized to the nucleus. At 3 or 4 dpf, live larvae were imaged using confocal microscopy. Larvae were then fixed with paraformaldehyde (PFA) in preparation for immunohistochemistry.

Antibody characterization

Anti-DsRed rabbit polyclonal antibody (Clontech, Mountain View, CA, #632496) was raised against DsRed-Express, a variant of *Discosoma sp.* red fluorescent protein. The quality and performance of this antibody was tested by Western blot analysis using lysates of HEK 293 cells stably expressing DsRed-Express, DsRed-Monomer, or AcGFP1 and untransfected HEK293 cells. A specific band corresponding to 30–38 kDa was observed only in lanes loaded with lysates of cells expressing DsRed-Express or DsRed-Monomer (manufacturer's technical information). In zebrafish, treatment of wild type fish with this antibody showed no positive signal (Fig. 1H).

A rabbit polyclonal Pax2 antibody (Invitrogen, #71-6000) was raised from a GST-Pax2 fusion protein derived from the C-terminal domain (aa188–385) of the murine Pax2 protein (Dressler and Douglas, 1992). Specificity of anti-Pax2 antiserum with zebrafish was discussed in detail in a previous study (Puschel et al., 1992). This antibody detects a protein of approximately 46 kDa in extracts from 24 hpf zebrafish embryos, as well as in extracts from mouse embryos.

A mouse monoclonal anti-GFP antibody (Invitrogen, #A-11120) was purified from clone 3E6 and recognizes native GFP (manufacturer's technical information). The specificity of this GFP antibody was confirmed by using *Isl1*-GFP fish (Higashijima et al., 2000). Immunostaining using this GFP antibody and the Alexa 598 anti-mouse IgG (1/500, Invitrogen) showed a complete overlap between the GFP fluorescence and the Alexa598 signal (data not shown).

Information on antibodies is summarized in Table 1.

Histology and immunohistochemistry

Fish were anesthetized with MS-222 and fixed with 4% PFA in 0.1 M phosphate buffer (PB, pH 7.2) at 4 °C for 5–7 hours. Samples were washed overnight with 30% sucrose in PB, followed by embedding with Tissue Tek OCT Compound (Sakura Finetech, Torrance, CA). Samples were then frozen and sectioned transversely (25 μ m) on a cryostat. Sections were

mounted on Superfrost Plus slides (Fisher) and dried. Slides were then washed in 0.1M PB for 30 minutes and coverslipped with Fluoromount-G (Southern Biotechnology Associates, Birmingham, AL).

Immunohistochemistry with anti-RFP was performed to emphasize DsRedExpress signals from fixed embryos. 24 hpf embryos were fixed with 4% PFA in 0.1 M PB overnight and then washed in 0.1 M PB for 5–7 hours. Samples were washed 2 times (10 minutes each) in phosphate buffered saline (PBS) containing 0.5% Triton X-100 (PBST) and then incubated in 100% ethanol followed by Acetone, at -20°C . After washing in PBST (2 times, 5 minutes each), samples were incubated in 2% normal goat serum (NGS) overnight at 4°C and in anti-DsRed antibody (1/2000) for 24 hours at 4°C . Samples were washed 3 times (2–3 hours each) in PBST and incubated overnight with secondary antibody, Alexa 568 goat anti-rabbit IgG (1/500, Invitrogen), at 4°C . After 3 washes in PBST, samples were observed with the confocal microscope.

For Pax2 immunohistochemistry, ventral trunk muscles of 3 dpf larvae were excised with a razor blade and treated with 1% collagenase (Sigma) for 20–30 minutes. Muscle cells and other tissues were removed to expose the spinal cord. The obtained spinal-fish were fixed with 4% PFA in 0.1 M PB and washed in 0.1 M PB as described previously. Samples were washed in PBST for 30 minutes and incubated in 2% NGS for 2–5 hours at room temperature. Samples were treated with rabbit polyclonal anti-Pax2 (1/400) for 12–60 hours at 4°C . In specimens expressing GFP, anti-GFP antisera (1/1000) were also added to the solution. Samples were washed 3 times (2–3 hours each) in PBST and incubated overnight with secondary antibodies, Alexa 488 goat anti-mouse IgG and Alexa 647 goat anti-rabbit IgG (1/500, Invitrogen). After 3 washes in PBST, samples were observed with the confocal microscope.

***In situ* hybridization**

The *pax8 in situ* probe was designed to target a 798bp region of the *pax8* transcript spanning exons 5 through 9 (Pfeffer et. al., 1998). The RFP probe was designed against DsRedExpress (700bp). *In situ* hybridization was carried out as previously described (Toyama et al.1995; Kudoh et. al 2001) with minor modifications. In brief, RNA probes were synthesized using a DIG RNA labeling Kit (SP6/T7) (Roche, Indianapolis, IN) following manufactures instructions. DIG labeled probes were purified with illustra ProbeQuant G-50 Micro Columns (GE Healthcare, Piscataway, NJ). *In situ* samples were fixed in 4% PFA in PBS overnight at 4°C . Following fixation, samples were washed with PBS, and transferred to methanol and stored at -20°C until processing. For processing, samples were rehydrated and treated with proteinase K (10mg/ml) for 7 minutes. Samples were then washed in PBS with 0.1% Tween-20 (PBTw) followed by fixation for 30 minutes at room temperature with 4% PFA in PBS. Samples were washed as before and then transferred to hybridization buffer (50% formamide, 5xSSC, 5mM EDTA, 0.1% Tween-20, 0.1% CHAPS, 50ug/ml heparin, 1mg/ml tRNA) and incubated at 65°C for 3 hours. Hybridization buffer was replaced with hybridization buffer containing $\sim 1\text{ng}/\mu\text{l}$ of probe and samples were incubated overnight. The optimal hybridization temperature for the Pax8 probe was 60°C and 62°C for the RFP probe. Following probe incubation samples were subjected to several rounds of washes with 4 separate buffers. Washing was followed by treatment with 2% blocking solution (Roche) containing 5% lamb serum (heat inactivated) for 1hour. Samples were then incubated overnight with anti-DIG-AP-Fab fragment antibody (Roche) at 4°C , optimal antibody dilution was determined for each probe. Color reaction was carried out using BM Purple AP Substrate (Roche) for 24h. Reaction was stopped with PBS and samples were fixed as before. Samples were then cleared and mounted in 75% glycerol and imaged with an Olympus MVX10 microscope.

Video imaging

Swimming analysis was performed as described in a previous study (Epley et al., 2008). In brief, high-speed video imaging was recorded with a 1024 PCI camera (TechImaging, Salem, MA) mounted on a Zeiss stereomicroscope Stemi 2000-C. Images were taken at the rate of 1000 frames/second. Sequential images were stored, and later processed in Photoshop. Swim pattern angles were analyzed using NIH ImageJ (NIH, Bethesda, MD). Rostral midlines were drawn in sequential images, within ImageJ, from these lines head tip and the angle were measured at individual time points.

Results

RFP gene was inserted in the *pax8* gene

Gene trap screening was performed using DsRedExpress for detection of insertion into the zebrafish genome. DsRedExpress is a mutant form of DsRed with altered amino acids at nine locations (Matz et al., 1999). While both DsRed and DsRedExpress require tetramerization to function as a RFP, the latter features a better solubility and a faster maturation of the chromophore (Bevis and Glick, 2002). The DsRedExpress sequence was positioned downstream of a splicing acceptor site, such that it would fuse to the endogenous transcript in the splicing process. DsRedExpress, with a splicing acceptor site, was flanked by Tol2. In the presence of transposase the flanking Tol2 sequences facilitate integration into the zebrafish genome (Fig. 1A). Fertilized zebrafish eggs were injected with a mixture of the Tol2-DsRedExpress construct and transposase mRNA, and were raised to adulthood. These adult fish were either in-crossed or out-crossed with wild type fish to screen for embryos that expressed RFP. A founder fish (F0) was identified that gave rise to offspring expressing RFP after ~20 hpf (Fig. 1C, G). The positive rate of embryos from this F0 fish was 1.5 % (3 embryos out of 206 embryos). Positive embryos were raised to adulthood, and out-crossed to generate F2 embryos. All experiments were done with F3 or later generations.

Using RFP (+) embryos as a template for inverse PCR, the site of RFP insertion was determined to be in the *pax8* gene. Further analysis mapped the insertion in the intron region between exons 1 and 2 (Fig. 1A). Previous studies have shown that *pax8* in zebrafish undergoes extensive alternative splicing (Mackereth et al., 2005). The zebrafish *pax8* gene has 13 exons, and alternative splicing gives rise to 10 different isoforms, with two predicted translation initiation sites.

We examined if the fusion of the DsRedExpress transcript and the *pax8* transcript occurred in the splicing process as predicted. We extracted mRNA from RFP (+) embryos, reverse-transcribed, and performed RACE PCR using reverse primers in the DsRedExpress sequence. From this PCR two amplicon bands were detected (Fig. 1B). Sequencing of these amplicons revealed the fusion of *pax8* and DsRedExpress. The inserted DsRedExpress sequence fused to either exon1a or 1c. When exon1a fuses to the DsRedExpress, the translation initiation site is the first methionine of DsRedExpress. Therefore, mRNA will lead to the expression of RFP. On the other hand, when exon1c fuses to the DsRedExpress, the translation initiation site in exon1c does not generate the DsRedExpress protein. In either case, fusion transcripts do not produce the Pax8 protein. Since the generation of the *pax8*-RFP fusion transcript is controlled by the innate transcription mechanism of *pax8*, RFP production is expected to serve as a faithful marker for *pax8*-lineage cells, as was reported in other gene trap lines (Tian et al., 2009).

To confirm that RFP expression follows the expression pattern of *pax8*, we performed *in situ* hybridization using probes for *pax8* and *RFP* and compared the staining pattern. The expression of *pax8* in wild type embryos (Fig. 2A, B) closely matched that of *RFP* in RFP

(+) embryos, both at 24 and 48 hpf (Fig. 2C–F). At 24 hpf, the expression of *RFP* in *pax8^{+/m}* and *pax8^{gm/m}* was detected in the midbrain-hindbrain boundary (mhb) region (Fig. 2C, E). At 48 hpf, the expression was observed also in the hindbrain region (Fig. 2D, F). This expression pattern was also observed in wild type samples probed with *pax8* (Fig. 2A, B). This similarity in expression pattern shows that *RFP* transcription indeed follows the intrinsic transcriptional regulation of the *pax8* gene and that the RFP fluorescence can serve as a marker of *pax8* expression in developing zebrafish embryos.

At 24 hpf, RFP expression was detected in the mhb and the otic vesicles (Fig. 1C, D). By 4 dpf, expression occurred in the mhb, hindbrain and the spinal cord (Fig. 1E, F). RFP expression in otic vesicles was hard to detect at this stage. Previous studies, employing *in situ* hybridization, showed the presence of *pax8* in the nephric duct (Pfeffer et al., 1998). However, due to the auto-fluorescence of the yolk sac, RFP signal in the surrounding area was obscured. This was alleviated by using immunohistochemistry with an anti-RFP antibody. Results revealed positive expression of RFP in the nephric duct (Fig. 1G) (Diep et al., in press). Wild type embryos treated with the same antibody do not show a positive signal in the same area (Fig. 1H). RFP immunohistochemistry also detected RFP expression in the eye (Fig. 1G). In the cross section of the eye, RFP expression was in the center of the retina and a positive signal was observed extending toward the brain (Fig. S1A), raising the possibility that retinal ganglion cells express RFP. However, confocal observation of a live fish indicated that a strong RFP signal was observed encircling the HuC-Cameleon-expressing optic nerve (Fig. S1B–G). HuC-Cameleon expressing retinal ganglion cells did not express RFP. This suggests that glial cells express *pax8*.

Fish homozygous for RFP insertion are Pax8 hypomorph

Using qPCR we examined if the insertion of the Tol2-RFP sequence was able to interfere with the endogenous expression of the *pax8* gene. Primers were designed to the junction between exons 5 and 6, to quantify normally-spliced transcripts in *pax8^{+/m}* or *pax8^{gm/m}* fish (Fig. 3A). The generation of amplicon was detected using a Taqman probe corresponding to the sequence encompassing the junction. At 1 dpf, the normal transcript in *pax8^{+/m}* fish was reduced to 52.8 ± 9.9 % of wild type fish (n=3, Fig. 3B). In *pax8^{gm/m}* fish it was further reduced to 3.1 ± 1.2 % of wild type fish (n=3). At 10 dpf, the amount of *pax8* transcript in wild type larvae was 41.9 ± 4.9 % compared to 1 dpf wild type embryos (n=3). *Pax8^{+/m}* or *pax8^{gm/m}* larvae also displayed reduced *pax8* levels: 29.5 ± 4.2 % and 2.1 ± 0.6 %, respectively (n=3; all values are relative to wild type transcript at 1 dpf; Average \pm SEM). An additional set of primers and probe, encompassing exons 7–8, was also tested and gave similar results (data not shown). In order to confirm the qPCR result, we compared *in situ* hybridization for *pax8* in *pax8^{+/+}*, *pax8^{+/m}* and *pax8^{gm/m}* embryos (Fig. 2). The signal was weaker in *pax8^{gm/m}* (Fig. 2A, G, H), and the decrease of transcript seems to happen uniformly among *pax8*-expressing cells. The *in situ* hybridization signal, however, was stronger than expected from the qPCR, presumably because the *pax8* probe can bind to the pre-mRNA.

In spite of the *pax8* ablation, the RFP expression pattern in *pax8^{gm/m}* fish (Fig. 3C, D) seemed similar to that of *pax8^{+/m}* fish (Fig. 1C, E). The overall structure of the brain was also normal in *pax8^{gm/m}* larvae (Fig. 3H, I). This was in contrast to a mutant of *pax2a*, a gene closely linked to *pax8*. *Pax2a* homozygous embryos exhibited a grossly deformed brain at 1 dpf, most notably the lack of isthmus and cerebellum (Brand et al., 1996). The *pax8^{gm/m}* fish did not display an obvious morphological defect (Fig. 3E, F, G) and followed a normal course of development to adulthood. (Fig. 3J). This was unexpected because *pax8* knockout mice present severe phenotypes and die soon after weaning (Mansouri et al., 1998).

The unexpected normal growth of *pax8^{gm/m}* fish raised a question whether Pax8 protein was indeed decreased as predicted by the mRNA measurements of qPCR (Fig. 3B). Previous studies of zebrafish reported that blocking of Pax8 by MO injection leads to an abnormal otic vesicle development (Hans et al., 2004; Mackereth et al., 2005). We looked at the formation of otic vesicles in *pax8^{gm/m}* fish. The size of otic vesicles in *pax8^{gm/m}* fish was slightly reduced at 1 dpf (Fig. 4A–C). The average area of otic vesicle was $5.79 \pm 0.51 \times 10^3 \mu\text{m}^2$ for wild type, $4.21 \pm 1.27 \times 10^3 \mu\text{m}^2$ for *pax8^{+/m}* and $2.57 \pm 0.38 \times 10^3 \mu\text{m}^2$ for *pax8^{gm/m}* (n=6; one-way ANOVA, $F_{(2,15)}=22.9$, $p<0.001$) (Fig. 4G). The reduction in the otic vesicle size became less pronounced as the larva gets older (Fig. 4D–F). The average area of otic vesicle at 10 dpf was $49.4 \pm 9.3 \times 10^3 \mu\text{m}^2$ for wild type, $42.8 \pm 5.9 \times 10^3 \mu\text{m}^2$ for *pax8^{+/m}*, and $39.1 \pm 6.5 \times 10^3 \mu\text{m}^2$ for *pax8^{gm/m}* (n=6; one-way ANOVA, $F_{(2,15)}=2.9$, $p=0.08$) (Fig. 4H).

To examine whether the smaller size of the otic vesicle results from the lack of *pax8*, we observed if *pax8* is expressed in the otic vesicle at 1 dpf. Because *in situ* hybridization signal of *pax8* at this stage was too weak to perform analysis (Fig. 2A), we used RFP as the marker to show putative *pax8* expressing cells. The otic vesicle had a cavity as revealed by Nissl staining. RFP expressing cells formed a layer that lined this cavity (Fig. 4I–K), which likely determines the size of the otic vesicle. Several groups reported that *pax8* regulates *pax2a* in the otic placode formation and together regulate the formation of otic vesicles (Hans et al., 2004; Mackereth et al., 2005). *In situ* hybridization of *pax8^{gm/m}* embryos with a *pax2a* probe, indeed revealed a reduced *pax2a* expression in the otic placodes at 14 hpf (Fig. 4L–O).

Finally, we generated a double mutant of *pax2a* and *pax8*, by making double-homozygous embryos for *pax8* and *no isthmus (noi)* (Brand et al., 1996). *Pax2a/pax8* double mutant embryos displayed a severely reduced otic vesicle size compared to single mutants of either *pax8* or *pax2a* (Fig. 4P–R). This again agrees with previous MO studies (Hans et al., 2004; Mackereth et al., 2005). Taken together, these results on the inner ear formation confirm the qPCR findings and that Pax8 function is inhibited in *pax8^{gm/m}*.

Expression of RFP in the nervous system

RFP expressing cells in the nervous system were examined in greater detail. Dorsal view of the hindbrain exhibited RFP (+) cells bilaterally (Fig. 5A). At higher magnification, axon-like structures crossing the midline were observed (Fig. 5B). In contrast to retinal expression (Fig. S1), RFP expressing cells also express HuC-Cameleon (data not shown). These observations suggest that RFP (+) cells in the hindbrain are mainly neurons. RFP (+) fish were also crossed with other transgenic lines to identify possible overlaps with RFP signals. *Is11*-GFP fish express GFP under the promoter of *Islet-1*, labeling GFP in cranial motor neurons (Higashijima et al., 2000). GFP/RFP double positive larvae showed that RFP (+) cells were distinct from GFP (+) motor neurons (Fig. 5C). They never overlapped, as shown clearly in a single confocal plane (Fig. 5D). After *in vivo* observation, GFP (+)/RFP (+) larvae were further examined in fixed slices (Fig. 5E–H). At the level of the IIIrd, Vth, VIIth, and Xth cranial motor nuclei, RFP (+) cells occupied distinct domains relative to motor neurons. When the reticulospinal neurons were stained with dextran fluorescein, there was no overlap with RFP expressing cells (Fig. 5I, J). RFP (+) cells were distributed more caudal than the 3rd segment. RFP (+) axons ascending to more rostral brain regions were not observed (data not shown). These results suggest that RFP (+) cells in the hindbrain include interneurons.

Pax2 and *pax8* in spinal interneurons

Though *pax8* is expressed in the zebrafish spinal cord, the role it plays in the spinal cord had remained unexplored, until recently. Batista and Lewis (2008) studied the expression of

pax8 along with *pax2a* in the spinal cord. While their findings suggested that the expression of these two genes largely overlaps, further characterization of *pax8*-expressing neurons was not performed. The better sensitivity of RFP fluorescence compared to *in situ* hybridization (Fig. 1, 2) enabled us to characterize putative *pax8*-lineage cells in the spinal cord.

The lateral view of a spinal cord in a *pax8^{+m}* fish expressing *isll*-GFP showed that RFP (+) cells were located in the dorsal spinal cord, distant from the motor neurons labeled by GFP (Fig. 6A). From the cell bodies of these RFP (+) neurons, axons extending ventrally could be visualized (Fig. 6B). In the ventro-lateral region, a plexus-like structure was observed, presumably arising from processes of RFP (+) cells (Fig. 6C). At the midline, RFP (+) fibers were observed near the ventral edge, that seemed to represent axons of commissural neurons (Fig. 6D).

We examined the overlap of Pax2a and RFP expression. We stained *pax8^{+m}* fish at 3 dpf with anti-Pax2 antibody. There were some cells expressing both Pax2a and RFP, which agrees with a report by Batista and Lewis (2008), but the overlap was not complete. In these stains there were also populations of neurons expressing only Pax2a or RFP (Fig. 6F). The Pax2a-expressing cells were overall shifted to the ventral side compared to the RFP (+) cells.

Because Circumferential Ascending interneurons (CiAs) express Pax2 (Batista and Lewis, 2008), we examined if CiAs also express RFP. To visualize CiA neurons in *pax8^{+m}* embryos, we injected a BAC clone with the *engrailed-1* (*eng1*) promoter driving GFP (Higashijima et al., 2004). *Eng1* is expressed exclusively in CiAs, and GFP driven by the *eng1* promoter labels CiAs efficiently. Among the GFP positive cells, CiA neurons were identified by their characteristic axon projection pattern (Fig. 6G). These CiA neurons were also further examined for RFP expression. Out of 11 CiA neurons identified by GFP, none displayed the expression of RFP (Fig. 6H, I). On the other hand, Pax2a was indeed expressed in CiA neurons (Batista and Lewis, 2008), evidenced by the anti-Pax2 signal in CiA (Fig. 6H, J). Therefore, CiA neurons express *pax2a*, but do not express RFP (*pax8*).

We next tried to determine the morphology of RFP (+) cells. Fibers visualized by RFP are too dense to allow morphological analysis of individual neurons (Fig. 6B). In order to visualize the morphology of RFP (+) neurons in isolation, a dye was injected into the spinal cord of *pax8^{+m}* fish (Hale et al., 2001). However, the efficiency of labeling RFP (+) cells with the dye was very low (data not shown). This data suggested that RFP (+) neurons do not extend long axons longitudinally. We therefore turned to a genetic method by injecting HuC-GFP or EF-GVP-Ulyn-UH2B constructs into *pax8^{+m}* embryos (Koster and Fraser, 2001). GFP expressed in a stochastic fashion enabled visualization of the axon morphology. By looking for cells positive for both GFP and RFP, we determined the morphology of RFP (+) cells. RFP (+) cells included Commissural Bifurcating Longitudinal interneurons (CoBLs), which extended axons contralaterally before bifurcating longitudinally (n = 11; Fig. 6K–M). We occasionally observed RFP (+) cells with shorter axons, which do not extend longitudinal after crossing midlines (n=2) or even do not cross the midline and remain in the ipsilateral side (n = 2) (data not shown). These cells may represent an undifferentiated form of CoBLs.

We also studied the expression of RFP in another class of inhibitory interneurons: Commissural Local interneurons (CoLos). These interneurons are glycinergic and extend axons that make connections onto contralateral motor neurons (Liao and Fetcho, 2008). An enhancer trap line expressing GFP in all CoLos, Tol-056, was recently reported (Satou et al., 2009). We crossed the RFP (+) fish with this enhancer trap line. GFP and RFP never

overlapped in these fish (Fig. 6N–P). In summary, RFP (+) cells were limited to a subclass of inhibitory neurons: CoBLs express RFP, but CiAs or CoLos do not.

The formation of spinal networks in *pax8* mutants

We examined the effect of inhibiting Pax8 on RFP (+) cells in the spinal cord, using *pax8^{gm/m}* fish. We first examined the expression of Pax2 and RFP in the spinal cord. The location and the density of Pax2 (+) cells or RFP (+) cells did not display an obvious change from those in *pax8^{+/m}* fish (Fig. 7A).

The morphology of RFP (+) neurons was examined in *pax8^{gm/m}* fish using the stochastic expression of GFP. RFP (+) neurons in these fish also included CoBLs. Axon morphology of the CoBL neurons (n = 8) did not show any obvious abnormalities (Fig. 7B).

The ostensible normal differentiation of CoBL neurons was further examined at the functional level. We compared the touch response behavior of *pax8^{gm/m}* larvae with that of wild type embryos. Larvae at 3 dpf were touched on the tail with a tungsten needle and the escape response was recorded under a high-speed camera. The escape response showed no obvious differences between wild type and *pax8^{gm/m}* larvae (Fig. 7D, G). For a greater detail comparison, movements of the rostral midline were measured (Fig. 7E, F, H, I) (Epley et al., 2008). The maximum angle for wild type (Fig. 7E) and *pax8^{gm/m}* (Fig. 7H) larvae was 138 ± 20 and 140 ± 24 respectively (n=5, average \pm SD, p=0.80, student's t-test). The peak angular velocity was 21.6 ± 1.4 and 21.4 ± 3.3 (p=0.90) (Fig. 7F, I). The duration was 11.2 ± 1.1 and 11.8 ± 1.3 (p=0.45). The normal escape response of *pax8^{gm/m}* fish, the smooth coordinated alternation of left-right excitation in particular, suggests that the networking of the spinal cord is maintained.

Spinal network formation in the *pax2a/pax8* double mutants

Lastly, we examined the spinal cord of *pax2a/pax8* double mutants (*pax2a^{-/-}pax8^{gm/m}* fish). Double mutants displayed a severe systemic phenotype. At 2 dpf, the edema started to develop (Fig. 8B). At 3 dpf, the edema became severe, most evident from the dorsal view (Fig. 8C, D). The survival of *pax2a^{-/-}* fish with different *pax8* genotypes (*pax8^{+/+}*, *pax8^{+/m}* and *pax8^{gm/m}*) was plotted against dpf (Fig. 8A). *Pax2a* single mutants die at ~10 dpf, as previously reported (Lun and Brand, 1998). When one or two mutant alleles of *pax8* were introduced, the survival of the fish was severely shortened.

In the double mutant, the RFP signal in the mhb was not observable at 1 dpf. This agrees with previous reports that *pax2* regulates the expression of *pax8* in the mhb (Liu and Joyner, 2001). In the spinal cord, RFP signal was visible but considerably weaker than that of *pax8* single-mutant fish (Fig. 9B). Due to the severe systemic abnormality at 3 dpf, the spinal cord of double mutant fish was observed at 2 dpf. At this stage, RFP (+) cells in the spinal cord were observed in the dorsal domain (Fig. 9D). However, the overall pattern of the RFP signal seemed different from control embryos. The network of processes arising from RFP (+) cells looked less dense. In order to analyze the specific change occurring at the single cell level, we turned to the stochastic expression of GFP; driven by *eng1-GFP*, *HuC-GFP* or *EF-GVP-Ulyn-UH2B*. We did not observe typical CoBLs in the double mutant. Instead, some RFP (+) cells differentiated into neurons that extended ipsilateral axons caudally (Fig. 8E–H). The morphology of these cells resembles that of Circumferential Ipsilateral Descending (CiD) interneurons or Ventral Lateral Descending (VeLD) interneurons (Batista et al., 2008). CiDs and VeLDs correspond to V2a and V2b neurons, respectively, in mammalian spinal cords. 3 out of 7 cells with ipsilateral descending axons were RFP (+). In wild type fish, nearly all CiD neurons arise from cells expressing the transcription factor *alx* (Kimura et al., 2006). We crossed RFP (+) fish with a stable transgenic line expressing *alx*-

GFP, in which the promoter of *alx* drives the expression of GFP and marks CiD with a high fidelity (Kimura et al., 2006). In these fish, the RFP signal and the GFP signal never overlapped (Fig. 9I, J). This shows that CiDs do not arise from RFP (+) cells in normal fish. Stochastically labeled neurons with ipsilateral descending neurons (n=10) were never observed to express RFP in *pax8^{gm/m}* fish. This suggests that VeLDs do not arise from the putative *pax8*-lineage either. The generation of RFP (+) neurons with ipsilateral descending axons in double mutant embryos therefore represents a change of cell fate in putative *pax8*-lineage neurons.

Discussion

In this study, we established a mutant zebrafish line that has an insertion of a RFP gene in the *pax8* gene. The novelties of this study are as follows: First, we used the gene trap technique in zebrafish to label a population of neurons as well as to inhibit the gene expression in the labeled neurons. Second, due to the time-dependent nature of the MO knockdown technique, the long-term effect of *pax8* loss in zebrafish was previously unknown. Thanks to the gene inhibition at the genomic level, we showed that *pax8*-less zebrafish survive to adulthood, unlike *pax8* knockout mice that die prematurely. Third, putative *pax8*-lineage neurons in the spinal cord were revealed to include CoBLs, but other inhibitory neurons including CiAs or CoLos do not arise from this population. Fourth, the *pax8/pax2* double mutant displayed a specific cell fate change of putative *pax8*-lineage neurons; they do not differentiate into CoBLs and instead give rise to neurons with ipsilateral descending axons.

The insertion of RFP in the *pax8* gene and the loss of Pax8 expression

The insertion of the RFP gene in *pax8* resulted in a fusion transcript. Due to the stop codon and the polyA addition signal that follows the RFP open reading frame, the expression of a functional Pax8 is inhibited. qPCR showed the expression level of *pax8* was, in fact, reduced to 2.5 % of wild type fish (Fig. 3B). This suppression of endogenous *pax8* is pronounced not only at 1 dpf but also at 10 dpf. The persistent suppression throughout development is due to the genomic nature of the RFP insertion. This is in contrast to earlier studies using MOs (Hans et al., 2004; Mackereth et al., 2005).

In spite of the nearly complete inhibition of the normal transcript in the *pax8* hypomorphic mutant, its phenotype was surprisingly mild. This mild phenotype was probably the reason why a random mutagenesis screening failed to isolate a mutant of *pax8*. Some teleost genomes have two duplicate genes corresponding to a single gene in mammals. It therefore raises the possibility that the zebrafish *pax8* gene has a duplicate copy that remains functional in *pax8^{gm/m}* fish. However, this is unlikely for four reasons. First, only a single gene homologous to *pax8* can be detected in the zebrafish genome database. Second, in the genome of *fugu rubripes*, another teleost species whose genome is completely sequenced, only a single copy of *pax8* exists (data not shown). Third, *pax8^{gm/m}* embryos presented a smaller otic vesicle size and reduced *pax2a* expression in the otic placode (Fig. 4). Fourth, *pax2a/pax8* double mutant displayed a much-reduced otic vesicle size (Fig. 4P–R) and an enhanced mortality rate compared to *pax2a* single mutant (Fig. 8A). Therefore, it is unlikely that a duplicate gene compensates for the inhibited *pax8* gene.

Pax8 expression in developing CNS

Previous studies in zebrafish used *in situ* hybridization to determine the timing and location of *pax8* expression (Pfeffer et al., 1998; Mackereth et al., 2005). However, some regions with a low level of *pax8* or RFP expression failed to exhibit *in situ* hybridization signals. For example, the otic vesicle at 24 hpf showed fluorescence but did not stain with *in situ*

hybridization (Fig. 1C, 2A). Similarly, RFP fluorescence detected in the spinal cord lacked matching *in situ* hybridization signals (Fig. 2D, 9A). The better sensitivity of the fluorescence signal enabled us to clarify the anatomical identity of *pax8*-expressing cells in the spinal cord for the first time.

On the other hand, there are some factors that need to be considered when interpreting the data. First, the time course of RFP may be delayed compared to the endogenous Pax8 expression, because RFP requires tetramerization and maturation before it starts to emit fluorescence. However, DsRedExpress, used in this study, has a much expedited maturation process compared to wild type DsRed (Bevis and Glick, 2002). Indeed, when compared to *in situ* hybridization with *pax8* or RFP specific probes, we did not observe a major delay in the expression of RFP fluorescence. Second, we needed to use *pax8*^{+/m} fish to observe RFP. In these fish, one allele of *pax8* is inhibited, as evidenced by qPCR (Fig. 3B). Therefore, there is a possibility that the morphology of cells expressing RFP in heterozygous fish may be different from that of *pax8*-lineage cells in wild type fish. However, the normal morphology of CiAs, CoBLs and CoLos in *pax8*^{+/m} or *pax8*^{m/m} fish (Fig. 6, 7) suggests it is unlikely. Third, while the nature of the RFP insertion in the *pax8* gene and the similarity of *pax8* and RFP *in situ* signals strongly support the validity of using RFP as the marker of *pax8*-lineage cells, a direct analysis of *pax8* expression using *in situ* hybridization in the spinal cord was impossible due to the weak signal. We refer to RFP (+) cells, used for the morphology analysis, as “putative” *pax8*-lineage cells to acknowledge this point.

The expression of Pax8 was detected in retina, mhb, hindbrain, spinal cord and nephric duct. In mammals, Pax8 was also found in the thyroid gland. *Pax8* knock-out mice die prematurely due to thyroid gland failure (Mansouri et al., 1998). Given the normal development of *pax8*^{m/m} fish, it will be an interesting question, in the future, to examine the function of thyroid hormones in zebrafish (Yonkers and Ribera, 2008).

Pax8 and Pax2a in the spinal cord

In the zebrafish genome, *pax2* has two duplicated copies: *pax2a* and *pax2b*. Only a mutant of *pax2a* (*noi*) was isolated in a large-scale mutagenesis screening. The interaction of *pax2a* and *pax8* in the zebrafish spinal cord was first studied by Batista and Lewis (2008). Based on the number of cells stained with single or double *in situ* hybridization, it was concluded that the expression of *pax2a*, *pax2b* and *pax8* largely overlap. It was also shown that *pax2a* neurons include CiAs. However, the identity of *pax8*-expressing interneurons was not studied. Our current study showed that the putative *pax8*-lineage neurons include CoBLs, but not CiAs or CoLos.

In mammalian spinal cord, *Pax2* (+) domains include V0, V1, dl4 and dl6 (Burrill et al., 1997; Pillai et al., 2007). *Alx* (+) areas and *eng1* (+) areas in zebrafish correspond to V2a and V1, respectively (Higashijima et al., 2004, Kimura et al., 2006). Areas of putative *pax8* (+) cells in zebrafish spinal cord are dorsal to *alx* (+) neurons (Fig. 9I), and partially overlap with the *pax2a* (+) domain (Fig. 6F). Some of the cell bodies, observed by RFP, without obvious axon extensions may be glias.

Our results from *pax8*^{m/m} embryos showed that CoBLs develop normally in *pax8* single mutants (Fig. 7). A MO study by Lewis et al. suggested that spinal neurons develop normally in *pax2a* single mutants (Batista and Lewis, 2008). We also observed CoBL neurons expressing RFP in *pax2a* single mutants (data not shown). In contrast to *pax8* or *pax2a* single mutants, *pax2a/pax8* double mutants showed a clear change of fate for RFP (+) interneurons in the spinal cord. The expression of transcription factors have been linked to specific populations of spinal neurons (Lewis, 2006); the knocking out of transcription factors leads to different effects in mammalian spinal cord. The knockout of *Dbx1* prevents

the formation of V0 neurons and leads to abnormal left-right alternation (Lanuza et al., 2004). In *engrailed1* knockout mice, a subpopulation of V1 neurons showed a subtler defect of reduced synaptic connection to target neurons (Sapir et al., 2004). Although RFP (+) cells in *pax2a/pax8* double mutants are positioned roughly in the correct domain of the spinal cord, their cell fate was clearly changed. First, the overall pattern of RFP (+) fibers was altered. Second, more remarkably, double mutants lead to the generation of neurons with ipsilateral descending axons from RFP (+) cells. We failed to identify CoBLs in double mutants, which we routinely encounter in control fish. Together with the altered pattern of plexus, it is likely that the CoBLs are absent in the double mutant. It also agrees with the previous report that in *pax2/pax8* knockdowns the development of inhibitory neurons is inhibited (Bastista and Lewis, 2008). RFP (+) neurons with ipsilateral descending axons that newly arose in the double mutant may represent CiDs, VeDLs or neither. The identity of these neurons awaits a further study.

An interesting question is how the motor output in the double mutant is affected by the cell fate change. This is difficult to address in the current study due to the poor health of the double mutants. The severe edema likely comes from defects in the mhb or the nephric duct. In the future, it will be interesting to partially rescue double mutants with mhb or nephric duct specific promoters (Gosgnach et al., 2006) and examine the effect of *pax2a/pax8* knockdown in the spinal cord in viable fish.

The analysis of the spinal interneuron network in zebrafish started from the anatomical classification based on the cell body location and the axon extension pattern (Bernhardt et al., 1990; Hale et al., 2001). Combination of genetic markers and electrophysiology made it possible to clarify functions that particular cell types display (Higashijima et al., 2004; Kimura et al., 2006; Liao and Fetcho, 2008; Satou et al., 2009). Use of MOs addressed the cell function from a different angle, by disturbing the development of specific interneurons (Batista and Lewis, 2008). The current study showed that the gene trap technique is a very powerful tool for such analyses; unequivocally labeling classes of interneurons expressing one type of transcription factor with a high sensitivity, while allowing the inhibition of its function in development. Generating more gene trap lines and combining them with other genetic techniques will further extend our understanding of the spinal cord network development.

Supplementary Material

Refer to Web version on PubMed Central for supplementary material.

Acknowledgments

We thank Drs Shinichi Higashijima and Joseph Fetcho for kindly providing *alx*-GFP fish, HuC-Cameleon fish, Tol-056 enhancer trap line, HuC-GFP construct, and *engrailed1*-GFP construct. We thank Drs Scott Fraser and Reiko Toyama for the EF-GVP-Ulyn-UH2B and *pax2a* clone respectively. We appreciate the technical advice from Drs Yu Katsuyama and Reiko Toyama on *in situ* hybridization. Dr. Kimberly Epley and Ms. Alison Delargy provided valuable help in maintaining zebrafish colonies. We thank Dr. Stephen Ikeda for critical reading of the manuscript.

Literature cited

- Batista MF, Lewis KE. Pax2/8 act redundantly to specify glycinergic and GABAergic fates of multiple spinal interneurons. *Dev Biol.* 2008; 323:88–97. [PubMed: 18761336]
- Batista MF, Jacobstein J, Lewis KE. Zebrafish V2 cells develop into excitatory CiD and Notch signalling dependent inhibitory VeLD interneurons. *Dev Biol.* 2008; 322:263–275. [PubMed: 18680739]

- Bernhardt RR, Chitnis AB, Lindamer L, Kuwada JY. Identification of spinal neurons in the embryonic and larval zebrafish. *J Comp Neurol.* 1990; 302:603–616. [PubMed: 1702120]
- Bevis BJ, Glick BS. Rapidly maturing variants of the Discosoma red fluorescent protein (DsRed). *Nat Biotechnol.* 2002; 20:83–87. [PubMed: 11753367]
- Bouchard M, Souabni A, Busslinger M. Tissue-specific expression of cre recombinase from the Pax8 locus. *Genesis.* 2004; 38:105–109. [PubMed: 15048807]
- Brand M, Heisenberg CP, Jiang YJ, Beuchle D, Lun K, Furutani-Seiki M, Granato M, Haffter P, Hammerschmidt M, Kane DA, Kelsh RN, Mullins MC, Odenthal J, van Eeden FJ, Nusslein-Volhard C. Mutations in zebrafish genes affecting the formation of the boundary between midbrain and hindbrain. *Development.* 1996; 123:179–190. [PubMed: 9007239]
- Burrill JD, Moran L, Goulding MD, Saueressig H. PAX2 is expressed in multiple spinal cord interneurons, including a population of EN1+ interneurons that require PAX6 for their development. *Development.* 1997; 124:4493–4503. [PubMed: 9409667]
- Chi N, Epstein JA. Getting your Pax straight: Pax proteins in development and disease. *Trends Genet.* 2002; 18:41–47. [PubMed: 11750700]
- Diep C, Ma D, Arora N, Wingert R, Bollig F, Djordjevic G, Lichman B, Zhu H, Ikenaga T, Ono F, Englert C, Hukriede N, Handin R, Davidson A. Identification of adult renal progenitor cells capable of nephron formation and regeneration in zebrafish. *Nature.* in press.
- Dressler GR, Douglas EC. Pax2 is a DNA-binding protein expressed in embryonic kidney and Wilms tumor. *Proc Natl Acad Sci U S A.* 1992; 89:1179–1183. [PubMed: 1311084]
- Epley KE, Urban JM, Ikenaga T, Ono F. A modified acetylcholine receptor {delta}-subunit enables a null mutant to survive beyond sexual maturation. *J Neurosci.* 2008; 28:13223–13231. [PubMed: 19052214]
- Ericson J, Rashbass P, Schedl A, Brenner-Morton S, Kawakami A, van Heyningen V, Jessell TM, Briscoe J. Pax6 controls progenitor cell identity and neuronal fate in response to graded Shh signaling. *Cell.* 1997; 90:169–180. [PubMed: 9230312]
- Erickson T, Scholpp S, Brand M, Moens CB, Waskiewicz AJ. Pbx proteins cooperate with Engrailed to pattern the midbrain-hindbrain and diencephalic-mesencephalic boundaries. *Dev Biol.* 2007; 301:504–517. [PubMed: 16959235]
- Friedrich G, Soriano P. Promoter traps in embryonic stem cells: a genetic screen to identify and mutate developmental genes in mice. *Genes Dev.* 1991; 5:1513–1523. [PubMed: 1653172]
- Gosgnach S, Lanuza GM, Butt SJ, Saueressig H, Zhang Y, Velasquez T, Riethmacher D, Callaway EM, Kiehn O, Goulding M. V1 spinal neurons regulate the speed of vertebrate locomotor outputs. *Nature.* 2006; 440:215–219. [PubMed: 16525473]
- Goulding M, Pfaff SL. Development of circuits that generate simple rhythmic behaviors in vertebrates. *Curr Opin Neurobiol.* 2005; 15:14–20. [PubMed: 15721739]
- Hale ME, Ritter DA, Fetcho JR. A confocal study of spinal interneurons in living larval zebrafish. *J Comp Neurol.* 2001; 437:1–16. [PubMed: 11477593]
- Hans S, Liu D, Westerfield M. Pax8 and Pax2a function synergistically in otic specification, downstream of the Foxi1 and Dlx3b transcription factors. *Development.* 2004; 131:5091–5102. [PubMed: 15459102]
- Higashijima S, Hotta Y, Okamoto H. Visualization of cranial motor neurons in live transgenic zebrafish expressing green fluorescent protein under the control of the islet-1 promoter/enhancer. *J Neurosci.* 2000; 20:206–218. [PubMed: 10627598]
- Higashijima S, Masino MA, Mandel G, Fetcho JR. Engrailed-1 expression marks a primitive class of inhibitory spinal interneuron. *J Neurosci.* 2004; 24:5827–5839. [PubMed: 15215305]
- Hutchinson SA, Eisen JS. Islet1 and Islet2 have equivalent abilities to promote motoneuron function and to specify motoneuron subtype identity. *Development.* 2006; 133:2137–2147. [PubMed: 16672347]
- Hutchinson SA, Cheesman SE, Hale LA, Boone JQ, Eisen JS. Nkx6 proteins specify one zebrafish primary motoneuron subtype by regulating late *islet1* expression. *Development.* 2007; 134:1671–1677. [PubMed: 17376808]
- Jessell TM. Neuronal specification in the spinal cord: inductive signals and transcriptional codes. *Nat Rev Genet.* 2000; 1:20–29. [PubMed: 11262869]

- Kawakami K, Takeda H, Kawakami N, Kobayashi M, Matsuda N, Mishina M. A transposon-mediated gene trap approach identifies developmentally regulated genes in zebrafish. *Dev Cell*. 2004; 7:133–144. [PubMed: 15239961]
- Kimura Y, Okamura Y, Higashijima S. *alx*, a zebrafish homolog of Chx10, marks ipsilateral descending excitatory interneurons that participate in the regulation of spinal locomotor circuits. *J Neurosci*. 2006; 26:5684–5697. [PubMed: 16723525]
- Koster RW, Fraser SE. Tracing transgene expression in living zebrafish embryos. *Dev Biol*. 2001; 233:329–346. [PubMed: 11336499]
- Kudoh T, Tsang M, Hukriede NA, Chen X, Dedekian M, Clarke CJ, Kiang A, Schultz S, Epstein JA, Toyama R, Dawid IB. A gene expression screen in zebrafish embryogenesis. *Genome Res*. 2001; 11:1979–1987. [PubMed: 11731487]
- Lanuzza GM, Gosgnach S, Pierani A, Jessell TM, Goulding M. Genetic identification of spinal interneurons that coordinate left-right locomotor activity necessary for walking movements. *Neuron*. 2004; 42:375–386. [PubMed: 15134635]
- Liao JC, Fetcho JR. Shared versus specialized glycinergic spinal interneurons in axial motor circuits of larval zebrafish. *J Neurosci*. 2008; 28:12982–12992. [PubMed: 19036991]
- Lun K, Brand M. A series of *no* isthmus (*noi*) alleles of the zebrafish *pax2.1* gene reveals multiple signaling events in development of the midbrain-hindbrain boundary. *Development*. 1998; 125:3049–3062. [PubMed: 9671579]
- Mackereth MD, Kwak SJ, Fritz A, Riley BB. Zebrafish *pax8* is required for otic placode induction and plays a redundant role with *Pax2* genes in the maintenance of the otic placode. *Development*. 2005; 132:371–382. [PubMed: 15604103]
- Mansouri A, Chowdhury K, Gruss P. Follicular cells of the thyroid gland require *Pax8* gene function. *Nat Genet*. 1998; 19:87–90. [PubMed: 9590297]
- Matz MV, Fradkov AF, Labas YA, Savitsky AP, Zarausky AG, Markelov ML, Lukyanov SA. Fluorescent proteins from nonbioluminescent Anthozoa species. *Nat Biotechnol*. 1999; 17:969–973. [PubMed: 10504696]
- O’Kane CJ, Gehring WJ. Detection in situ of genomic regulatory elements in *Drosophila*. *Proc Natl Acad Sci U S A*. 1987; 84:9123–9127. [PubMed: 2827169]
- Ono F, Higashijima S, Shcherbatko A, Fetcho JR, Brehm P. Paralytic zebrafish lacking acetylcholine receptors fail to localize rapsyn clusters to the synapse. *J Neurosci*. 2001; 21:5439–5448. [PubMed: 11466415]
- Pfeffer PL, Gerster T, Lun K, Brand M, Busslinger M. Characterization of three novel members of the zebrafish *Pax2/5/8* family: dependency of *Pax5* and *Pax8* expression on the *Pax2.1* (*noi*) function. *Development*. 1998; 125:3063–3074. [PubMed: 9671580]
- Pillai A, Mansouri A, Behringer R, Westphal H, Goulding M. *Lhx1* and *Lhx5* maintain the inhibitory-neurotransmitter status of interneurons in the dorsal spinal cord. *Development*. 2007; 134:357–366. [PubMed: 17166926]
- Puschel AW, Westerfield M, Dressler GR. Comparative analysis of *Pax-2* protein distributions during neurulation in mice and zebrafish. *Mech Dev*. 1992; 38:197–208. [PubMed: 1457381]
- Sapir T, Geiman EJ, Wang Z, Velasquez T, Mitsui S, Yoshihara Y, Frank E, Alvarez FJ, Goulding M. *Pax6* and *engrailed 1* regulate two distinct aspects of *renshaw* cell development. *J Neurosci*. 2004; 24:1255–1264. [PubMed: 14762144]
- Satou C, Kimura Y, Kohashi T, Horikawa K, Takeda H, Oda Y, Higashijima S. Functional role of a specialized class of spinal commissural inhibitory neurons during fast escapes in zebrafish. *J Neurosci*. 2009; 29:6780–6793. [PubMed: 19474306]
- Segawa H, Miyashita T, Hirate Y, Higashijima S, Chino N, Uyemura K, Kikuchi Y, Okamoto H. Functional repression of *Islet-2* by disruption of complex with *Ldb* impairs peripheral axonal outgrowth in embryonic zebrafish. *Neuron*. 2001; 30:423–436. [PubMed: 11395004]
- Tian T, Zhao L, Zhao X, Zhang M, Meng A. A zebrafish gene trap line expresses GFP recapturing expression pattern of *foxl1b*. *J Genet Genomics*. 2009; 36:581–589. [PubMed: 19840756]
- Toyama R, O’Connell ML, Wright CV, Kuehn MR, Dawid IB. *Nodal* induces ectopic *goosecoid* and *lim1* expression and axis duplication in zebrafish. *Development*. 1995; 121:383–391. [PubMed: 7768180]

- Treisman J, Harris E, Desplan C. The paired box encodes a second DNA-binding domain in the paired homeo domain protein. *Genes Dev.* 1991; 5:594–604. [PubMed: 1672661]
- Yonkers MA, Ribera AB. Sensory neuron sodium current requires nongenomic actions of thyroid hormone during development. *J Neurophysiol.* 2008; 100:2719–2725. [PubMed: 18799597]

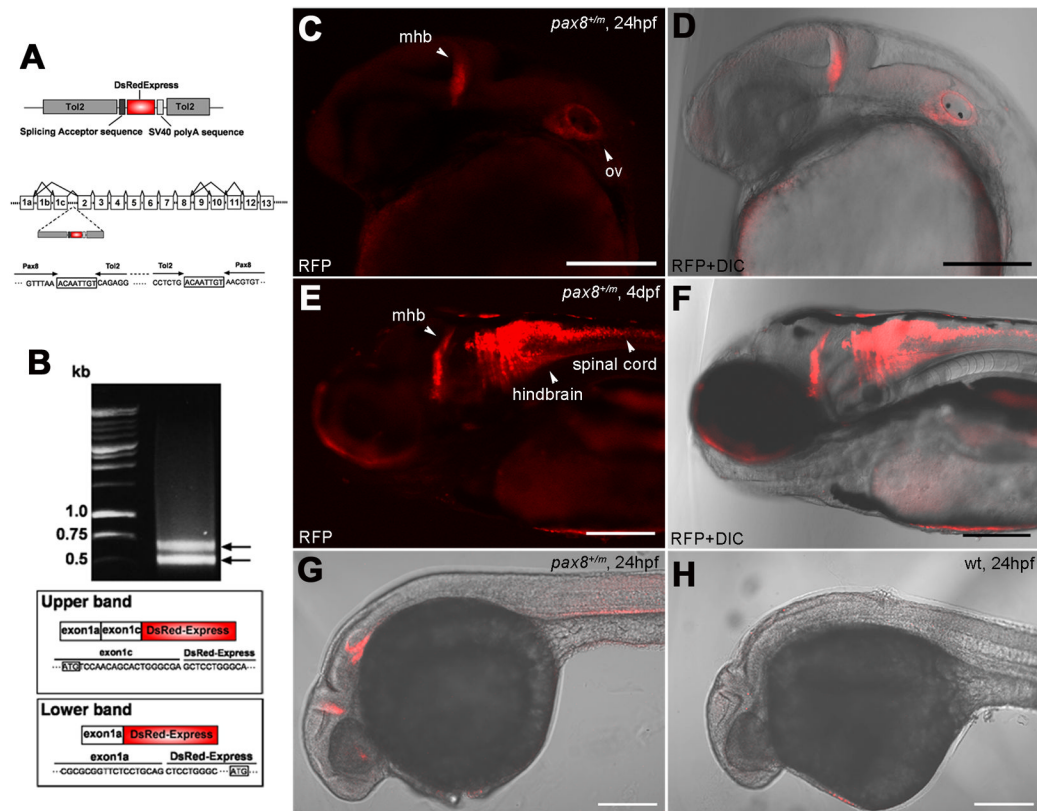


Figure 1. Insertion of RFP in the *pax8* gene leads to RFP expression. **A:** A schematic diagram of the DNA construct used in the gene trap screening (top). The construct has a splicing acceptor site, DsRedExpress sequence and the SV40 polyA sequence. Tol2 sequences are at both ends. Exon composition of the *pax8* gene in zebrafish is shown with possible alternative splicing combinations (middle). The insertion of the Tol2 sequence was detected in the first intron between exons 1c and 2. The nucleic acid sequence surrounding junctions is shown (bottom). Note the repeat of eight nucleic acids at both ends of the insertion, a phenomenon commonly observed with the Tol2 insertion. **B:** An electrophoresis image of RACE PCR products. Two distinct bands were detected. The upper band corresponded to the splicing of exons 1a+1c and DsRed, while the lower band corresponded to the splicing between exon 1a and DsRed. Presumptive translation initiation site for each transcript is shown with a box. **C, D:** Confocal image of RFP signal in *pax8^{+m}* embryos at 24 hpf (**C**). The signal is detected at the midbrain-hindbrain boundary (mhb) and the otic vesicle (ov). **D** shows the merged image with transmitted light. Scale: 200 μ m. **E, F:** At 4 dpf, the signal is detected also in the hindbrain and the spinal cord. **F** is the merged image with transmitted light. Scale: 200 μ m. **G, H:** RFP antibody stains the mhb, otic vesicle and the kidney at 24 hpf (**G**). **H** is a wild type embryo control. Scale: 200 μ m.

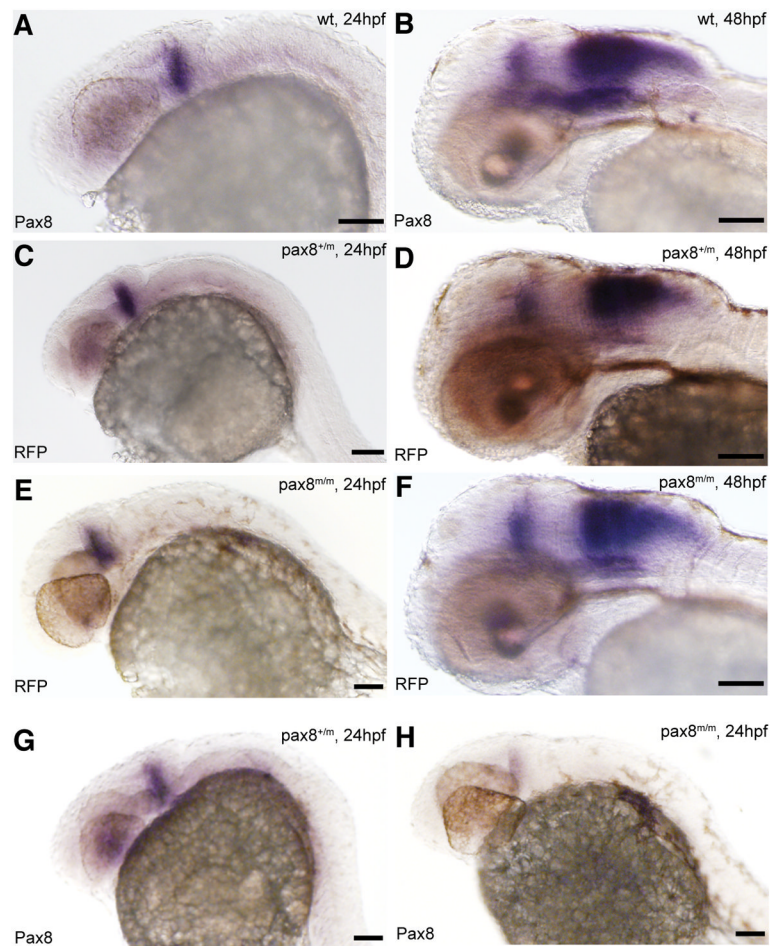


Figure 2. *Pax8* expression is identical to *RFP* expression. Transcripts were detected using *in situ* hybridization with either *pax8* (A, B, G, H) or *RFP* (C, D, E, F) probes in 24hpf (A, C, E, G, H) or 48hpf (B, D, F) embryos. Expression pattern, at 24hpf, of *pax8* in wild type (*pax8*^{+/+}, A) was same to that of *RFP* in *pax8*^{+/m} (C) and *pax8*^{m/m} (E). Signal was detected in the mhb region of the embryos. *RFP* showed no signal in wild type samples (data not shown). At 48hpf the staining pattern of *pax8* in wild type (B) resembled that of *RFP* expression in *pax8*^{+/m} (D) and *pax8*^{m/m} (F) embryos. *Pax8*^{+/m} embryos showed positive staining also with the *pax8* probe (G). *Pax8* transcripts were also detected, at a much lower intensity, in *pax8*^{m/m} embryos (H). Scale: 100 μ m.

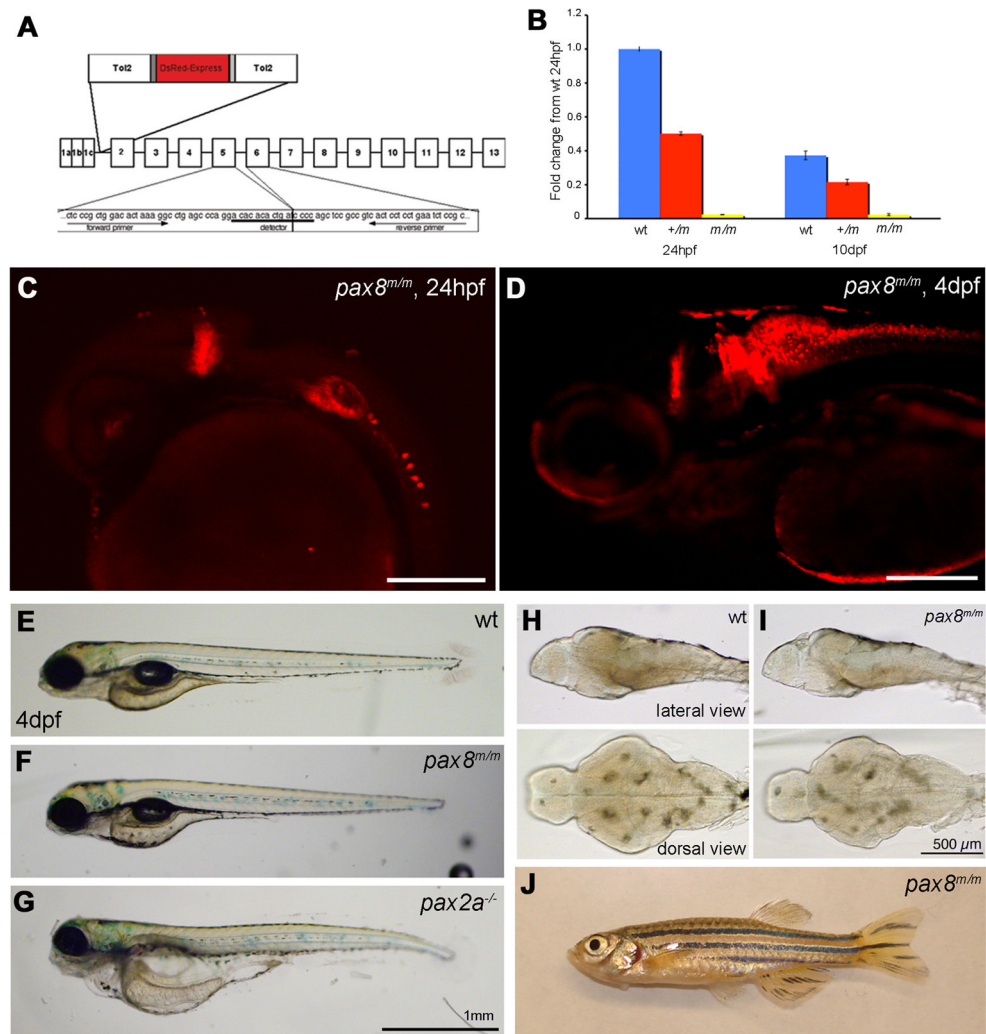


Figure 3. Homozygous embryos are Pax8 hypomorph. **A:** The exon composition of zebrafish *pax8* indicating the insertion site of Tol2. Primers for the qPCR were designed so that the amplicon spans the junction between exons 5 and 6. **B:** qPCR of the *pax8* transcript in wild type (wt), *pax8^{+/m}*, and *pax8^{m/m}* fish at 1 dpf and 10 dpf. Wild type at 1 dpf was used as a reference sample to obtain relative transcript amounts. Error bars represent the SEM of the average from triplicates of a single run (n=3). **C, D:** Confocal images of RFP signals in *pax8^{m/m}* fish at 24 hpf (**C**) and 4 dpf (**D**). Scale: 200 μ m. **E, F, G:** The gross morphology of larva at 4 dpf. **E** is wild type, **F** is *pax8^{m/m}*, and **G** is *pax2a^{-/-}*. The *pax2a^{-/-}* larva is deformed, and dies at 7–10 dpf. Scale: 1 mm. **H, I:** The brain morphology is normal in the *pax8^{m/m}* larva (**I**) compared to the WT larva (**H**). Top is the lateral view and bottom is the dorsal view. Scale: 500 μ m. **J:** Adult *pax8^{m/m}* fish.

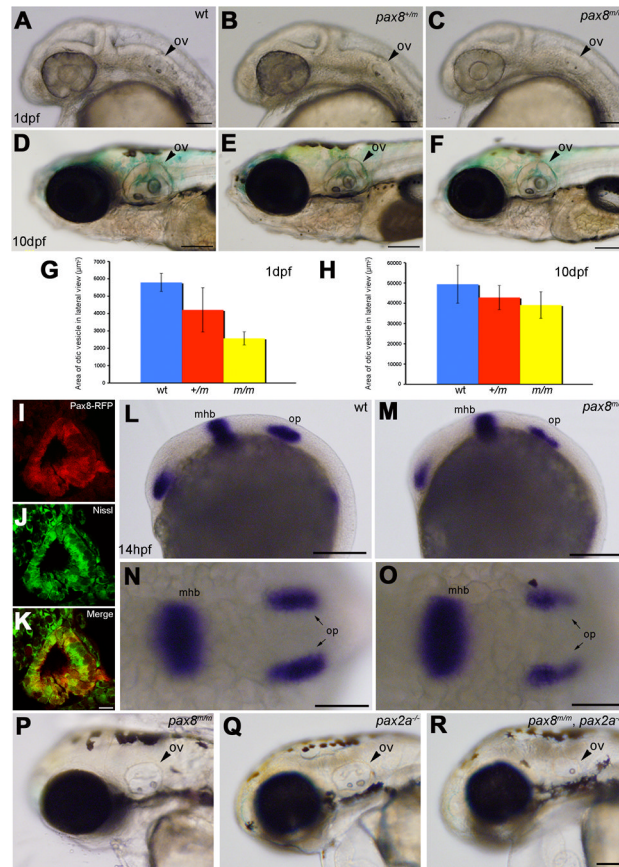


Figure 4.

Otic vesicle formation defects in *pax2a/pax8* mutants. **A–F:** The otic vesicle (ov) size is slightly reduced in *pax8^{m/m}* fish. Lateral view of the head region at 1 dpf (**A, B, C**) and 10 dpf (**D, E, F**). **A** and **D** are the wild type (wt), **B** and **E** are *pax8^{+/m}*, and **C** and **F** are *pax8^{m/m}*. Scale: 100 μ m (**A, B, C**), 200 μ m (**D, E, F**). **G, H:** The area of the otic vesicle as measured in the lateral view at 1 dpf (**G**) and 10 dpf (**H**). Wild type (Blue), *pax8^{+/m}* (Red), and *pax8^{m/m}* fish (Yellow). The average and the standard deviation are shown (n=6 each). **I, J, K:** C. RFP (+) cells (**I**) line the cavity of the otic vesicle, as visualized by the Nissle counterstain (**J**) at 1 dpf. The merged picture is shown in **K**. Scale 10 μ m. **L–O:** *In situ* hybridization with *pax2a* probes in wild type (**L, N**) and *pax8^{m/m}* embryos (**M, O**) at 14 hpf. *Pax2a* expression is detected in retina, mhb and the otic placode (op) in wild type. Note the signal in the otic placode is weaker in *pax8^{m/m}* embryo. The difference is more obvious in the higher magnification of the dorsal view (**N** and **O**). Scale: 200 μ m (**L, M**), 100 μ m (**N, O**). **P, Q, R:** The reduction of the otic vesicle size is more pronounced in the *pax2a/pax8* double mutant. The lateral view of the head is shown for *pax8^{m/m}* (**P**), *pax2a^{-/-}* (**Q**) and *pax2a/pax8* double mutant embryos at 2 dpf (**R**). Scale: 100 μ m. Magenta/green images for panels I, J and K are provided in suppl. figure. 2.

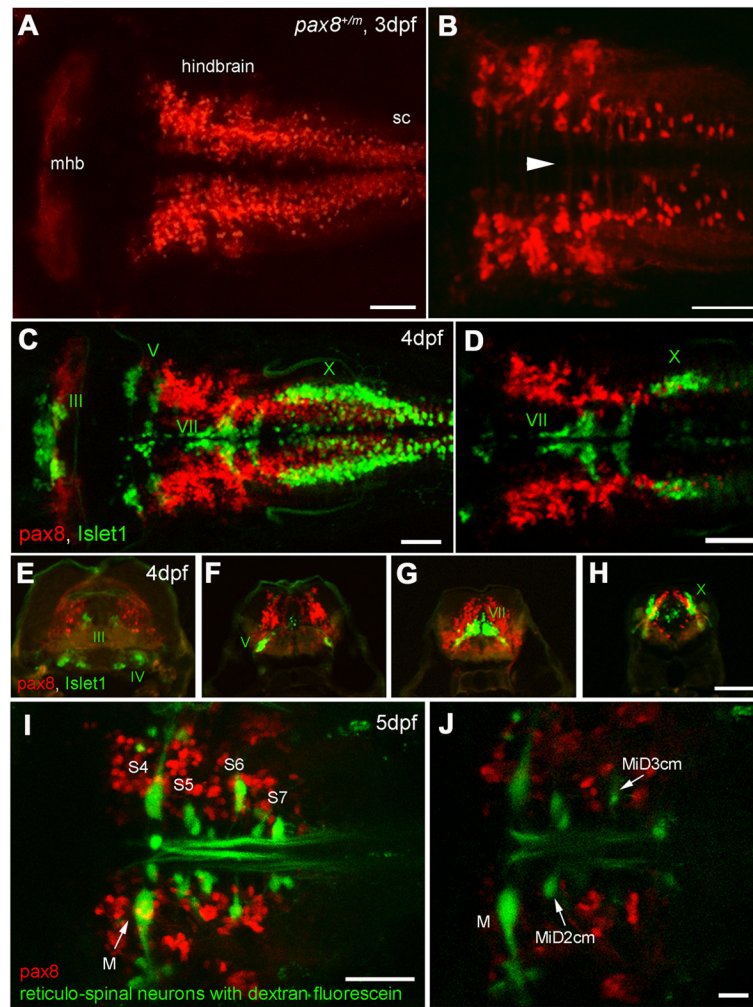
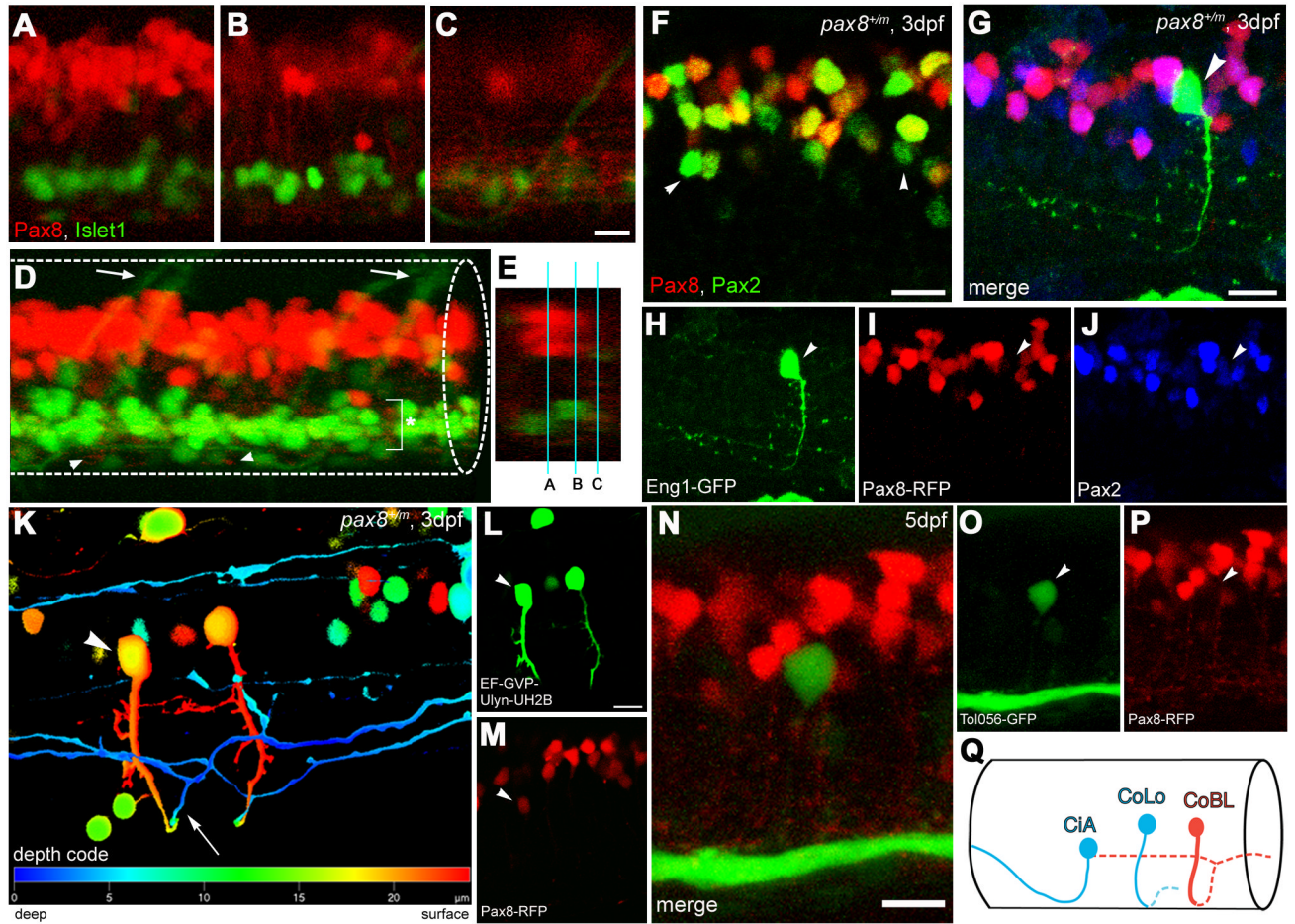


Figure 5.

RFP expression in the central nervous system. **A, B:** Confocal images displaying RFP (+) cells in the hindbrain. **A** is a dorsal view of the hindbrain and **B** is a higher magnification of the ventral region. Note the rostral end of the hindbrain lacks RFP (+) cells (**A**). In the ventral region (**B**), axon-like structures were detected crossing the midline (arrowhead). sc, spinal cord. Scale: 50 μm . **C, D:** RFP (+) cells (red) in the hindbrain compared to the *islet-1* GFP expressing motor neurons (green). **C** is a stack of confocal images. **D** displays a single confocal plane near the Xth (X) motor nuclei. Note that two populations (red and green) do not overlap. Scale: 50 μm . **E-H:** A longitudinal series of the hindbrain sections are shown from the level of IIIrd, IVth (**E**), Vth (**F**), VIIth (**G**), and Xth motor nucleus (**H**). RFP (+) cells are red and *islet-1* expressing motor neurons are green. Scale: 100 μm . **I, J:** RFP (+) cells (red) in the hindbrain were compared to the reticular neurons stained by the tracing dye, dextran fluorescein (green). **I** is a stack of confocal images and **J** is a single plane at the level of the Mauthner cell (M). S4 through S7 indicates segment number. Scale: 50 μm (**I**), 20 μm (**J**). Magenta/Green images are provided in suppl. figure. 3.

**Figure 6.**

Interneurons in the spinal cord expressing *pax2a* or *pax8*. **A-E**: RFP (+) neurons are detected in the dorsal portion of the spinal cord; RFP (red), *islet-1*:GFP (green). Single plane confocal images (**A**, **B**, **C**) show the position of RFP(+) cells and *islet-1* expressing secondary motor neurons. Scale: 10 μm . **D** is the 3D reconstruction. Arrowheads indicate commissural axons labeled by RFP and arrows indicate motor neuron axons labeled by GFP. The area with an asterisk has a plexus-like structure of RFP (+) fibers. An optical cross section (**E**) displays the level of confocal planes corresponding to **A**, **B** and **C**. **F**: *Pax8^{+/m}* fish stained with anti-Pax2; RFP (red), anti-Pax2 (green). Arrowheads are Pax2 (+) cells without RFP. Scale: 10 μm . **G-J**: CiA neurons express Pax2 but lack RFP expression. **G** is a stack of confocal images with *eng1*-GFP (green), RFP (red) and Pax2 (blue). **H-J** are single plane images to show that the GFP (+) cell is Pax2 (+) but RFP (-). Scale: 10 μm . **K, L, M**: CoBL neurons express RFP. **K** is a stack of confocal images in depth coding. The cell with an arrow has the characteristic axon pattern of CoBL. In single planes, the GFP (+) cell is also RFP (+) (**L** and **M**). Scale: 10 μm . **N, O, P**: CoLo neurons labeled with GFP (green) in Tol-056 fish do not express RFP (red). **N** is a merged image. **O** and **P** show that the marked cell expresses GFP but not RFP. Scale: 10 μm . **Q**: Schema of CiA, CoLo and CoBL interneurons in the spinal cord. The position of the cell body and the axon projection are shown. Rostral to the left. Note that CiA and CoLo (blue) do not express RFP, while CoBL (red) express RFP. Magenta/Green images are provided in suppl. figure. 4.

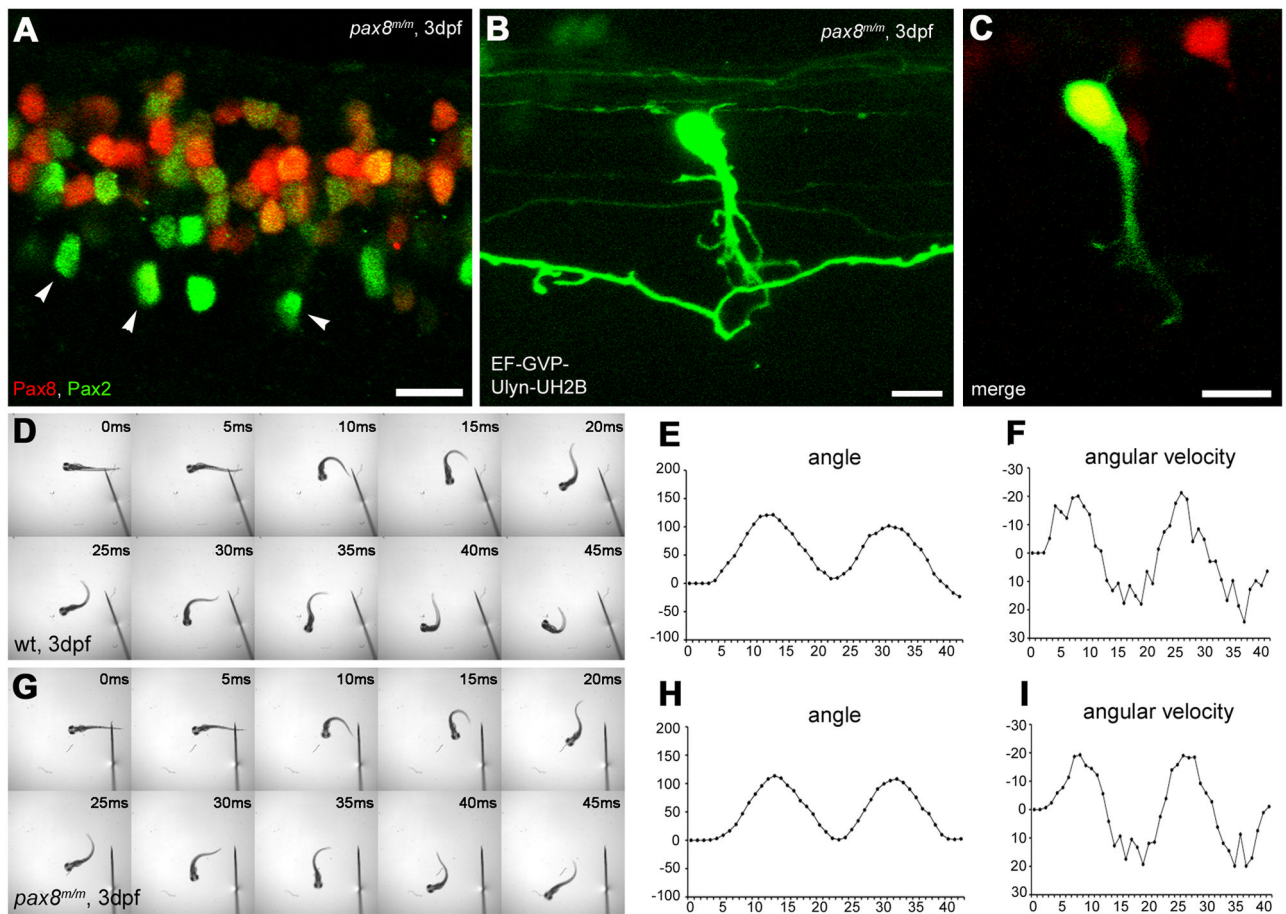


Figure 7.

Spinal neurons in *pax8* mutant. **A:** Spinal cord of a *pax8^{m/m}* fish stained with anti-Pax2; RFP (red), anti-Pax2 (green). Scale: 10 μ m. **B, C:** CoBL cell in *pax8^{m/m}* fish. B is a stack of confocal images and C is a single confocal plane; GFP (green), RFP (red). Scale: 10 μ m. **D–I:** Touch response of wild type (top, **D, E, F**) and *pax8^{m/m}* fish (bottom, **D, G, H, I**) at 3 dpf. High-speed images of escape response are shown from 0 ms to 45 ms (**D, G**). In **E, F, H, I**, the head angle (**E, H**) and the angular velocity (**F, I**) were plotted against time. Magenta/Green images of panels A, B and C are provided in suppl. figure. 5.

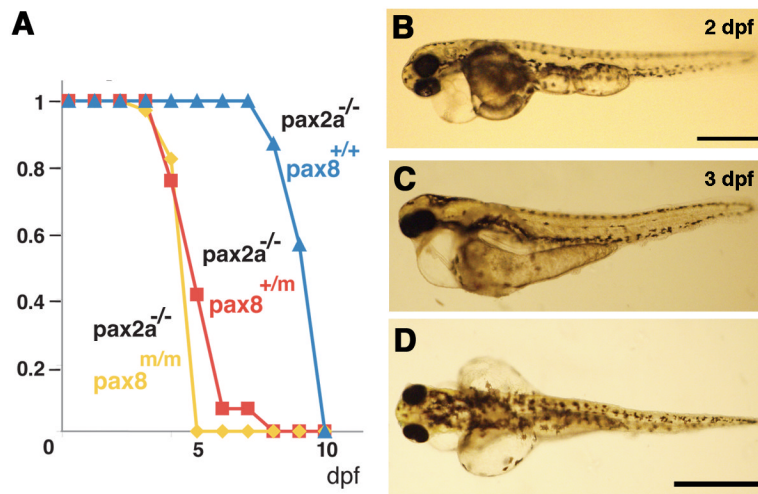


Figure 8. *Pax2a/pax8* double mutant. **A:** Survival curve of *pax2a* mutants with different *pax8* genotypes. Blue, red and yellow represents *pax8*^{+/+}, *pax8*^{+/m}, *pax8*^{m/m} fish, respectively. **B:** Lateral view of a double mutant embryo at 2 dpf. Scale: 500 μ m. **C, D:** Lateral (**C**) and dorsal (**D**) view of a 3 dpf double mutant larvae. Scale: 1 mm.

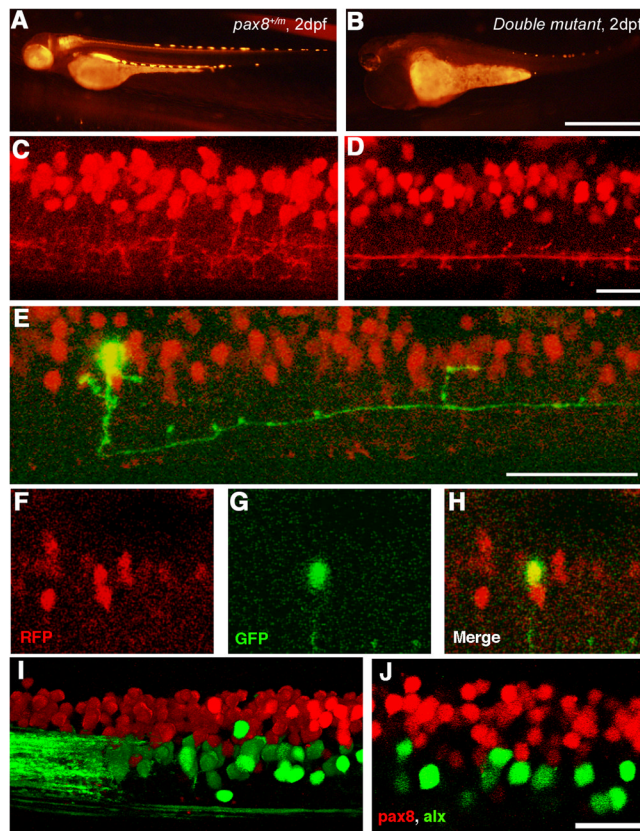


Figure 9. Spinal neurons in *pax2a/pax8* double mutant. **A, B:** RFP fluorescence of a *pax8^{+/m}* embryo (**A**) and a double mutant embryo (**B**) under the same optical condition. The RFP signal is reduced in the double mutant. Scale: 1 mm. **C, D:** The RFP signal in the spinal cord of a *pax8^{+/m}* embryo (**C**) and a double mutant embryo (**D**) near the 15th body segment. 3D images were constructed from confocal slices. Scale: 20 μ m. **E–H:** Stochastic labeling by GFP (green) identified a neuron with an ipsilateral descending axon in the double mutant. **E** is a 3D reconstruction. **F** (RFP), **G** (GFP), and **H** (merged) are single plane images. Scale: 50 μ m. **I, J:** The spinal cord of a *pax8^{+/m}* larva obtained from crossing with the Alx-GFP transgenic line. The image is from an embryo at 4 dpf. **I** is a 3D reconstruction and **J** is a single confocal plane. Note that RFP and GFP do not overlap. Scale: 20 μ m. Magenta/Green images are provided in suppl. figure. 6.

Table 1

Antibody characteristics

Antigen	Immunogen	Manufacturer	Dilution
DsRed	DsRed-Express, a variant of <i>Discosoma sp.</i> red fluorescent protein	Clontech (Mountain View), rabbit polyclonal, #632496	1:2,000
Pax2	GST-Pax2 fusion protein derived from the C-terminal domain (aa188–385) of the murine Pax2 protein	Invitrogen (Eugene), rabbit polyclonal, #71-6000	1:400
Green Fluorescent Protein (GFP)	Green fluorescent protein purified from <i>A. victoria</i>	Invitrogen (Eugene), mouse monoclonal, clone 3E6, #A- 11120	1:1,000